Effect of Local Chain Conformation in Adsorbed Nanolayers on Confined Polymer Molecular Mobility

Biao Zuo,[1,2,‡] Hao Zhou,[1] Mary J. B. Davis,[2] Xinping Wang,[1,*] and Rodney D. Priestley[2,3,†]
[1]Department of Chemistry, Zhejiang Sci-Tech University, Hangzhou 310018, China
[2]Department of Chemical and Biological Engineering, Princeton University, Princeton, New Jersey 08544, USA
[3]Princeton Institute for the Science and Technology of Materials, Princeton University, Princeton, New Jersey 08544, USA

(Received 29 January 2019; published 29 May 2019)

Interfaces play an important role in modifying the dynamics of polymers confined to the nanoscale. We demonstrate that the distance over which an interface suppresses molecular mobility in poly(styrene) thin films can be systematically increased by tens of nanometers by controlling the chain of conformation, i.e., the height of the loops in irreversibly adsorbed nanolayers. These effects arise from topological interaction between adsorbed and neighboring unadsorbed chains, respectively, which increase their motional coupling to facilitate the propagation of suppressed dynamics originating at the interface, thus highlighting the ability to manipulate interfacial effects by local conformation of chains in adsorbed nanolayers.

DOI: 10.1103/PhysRevLett.122.217801

The dynamics of polymers confined to the nanoscale are different from those of the bulk [1–8]. Consensus is emerging that interfaces, which can alter the conformation of nearby chains, are the underpinnings of confinement effects on molecular dynamics [2–5]. Modified dynamics at the interface can propagate over a length scale of tens of nanometers [6–8], creating a percolation network which alters average mobility [9,10]. Hence, understanding the pathway by which interfacial mobility propagates within confined polymers is of critical importance. Moreover, our ability to harness such effects, by systematically controlling the length scale over which modified dynamics propagate away from the interface, would provide a unique means to exploit confinement to tune polymer properties.

Irreversibly adsorbed nanolayers, immobilized ultrathin layers of polymers strongly adhered atop a solid surface, are worthy of special attention because their structure and properties are crucial to how interfacial effects impact thin film dynamics. Napolitano and co-workers [11–14] demonstrated that substrate effects on the glass transition temperature (T_g) and segmental dynamics, measured in thin films upon confinement, could be directly related to the degree of chain adsorption at the substrate. Koga *et al.* [15] and Wang and co-workers [16–18] revealed that suppressed dynamics of ultrathin adsorbed layers could extend tens of nanometers away from the substrate, which could be related to the thickness or architecture of the adsorbed layer. Meanwhile, Burroughs *et al.* found that such layers have an enhanced T_g [19]. It has been proposed that absorbed layer effects on molecular mobility are realized by topological interactions between structures within adsorbed chains, i.e., loops, and those of neighboring unadsorbed chains in a matrix, which ensure continuity in the mobility gradient emanating from the substrate and ending in the bulk [20,21], thus further underscoring the importance of the conformations of the adsorbed chains to the long-range interfacial effects.

Referring to the conformations of chains in the adsorbed layers, earlier theoretical works predicted that chains adsorbed atop a solid surface adopt conformations in the form of loops, trains, and tails [22,23]. Recently, Koga and co-workers [24,25] experimentally revealed that chains in tightly bound adsorbed layers (also known as flattened layers or bound loop layers [26]) mainly adopted a closely arranged loop conformation with high-density segment-solid contacts to achieve large enthalpic gains. The concrete picture obtained from its structure now enables the precise design of the adsorbed layers. In this Letter, we exploit such a design to illustrate that the size of loops in the flattened adsorbed layers is a key parameter that controls the propagation of suppressed interfacial dynamics—and accordingly the dynamics—of polymer thin films.

Here, we used a random copolymer of poly (styrene-*ran*-4-hydroxystyrene) P(S-r-HS) [see Figs. S1–S3 and Table S1 in the Supplemental Material (SM) [27] for details of the synthesis] to prepare adsorbed layers atop silicon wafers with native oxide layers. Note that the similar reactivity ratios between S and HS ensure the formation of a statistical copolymer [31,32]. Since HS has a greater affinity to the silicon surface through OH-OH interactions [33], it will preferentially adsorb atop it over the S components in the copolymer, thus providing a means to generate loops in the flattened nanolayers. Control of the loop height of the flattened chains was achieved by changing the mole fraction (f_{HS}) of HS in the copolymer. To obtain adsorbed layers, spin-coated films of P(S-r-HS) ($h = 80 \pm 2$ nm) were annealed at 443 K for 3 h under vacuum and then solvent leached using propylene glycol

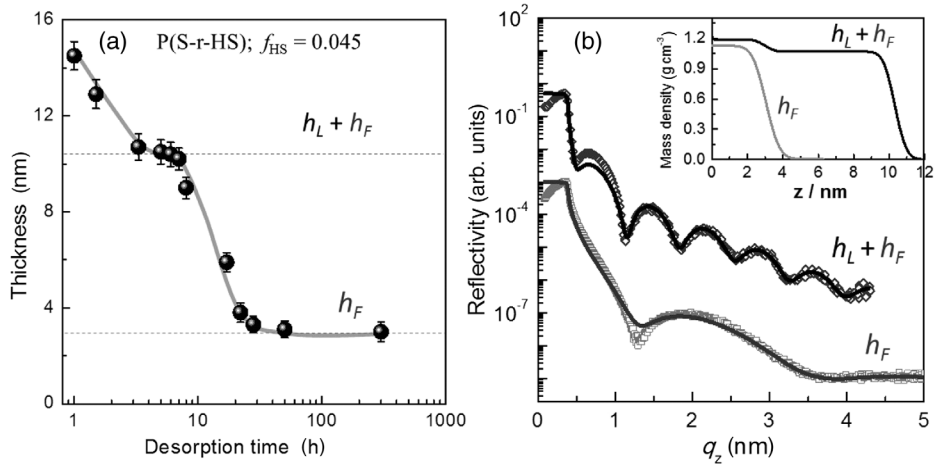

FIG. 1. (a) Thickness of residual layers of P(S-r-HS) as a function of solvent-leaching time. (b) XRR curves of the adsorbed layers consisting of the loosely adsorbed layers (h_L) and flattened layers (h_F), and of h_F only. (Inset) The density profile of the adsorbed layers.

methyl ether acetate (i.e., a good solvent for both PS and PHS) to remove the nonadsorbed chains. The residual layers were dried under vacuum at 393 K for 1 h and then characterized by ellipsometry, x-ray reflectivity (XRR) and AFM.

Figure 1(a) presents the thickness of the residual film of P(S-r-HS) with $f_{HS} = 0.045$, assessed by ellipsometry and XRR, as a function of solvent-leaching time. Notably, two plateaus at thicknesses of 10.4 and 3.0 nm were clearly observed. We note that the two-step desorption behavior was previously reported and interpreted by Gin *et al.* [24] and is indicative of the existence of two different architectures within adsorbed layers: inner flattened chains constituted by regularly arranged loops (i.e., flattened layers), and loosely adsorbed outer chains with fewer contacts with the substrate. During solvent leaching between 3 h $< t <$ 8 h, the exposed adsorbed layers consisted of both flattened and loosely adsorbed chains with thickness of ~10.4 nm. For solvent leaching $t >$ 24 h, the second plateau exposed a 3.0 nm thick absorbed layer consisting only of flattened chains. Results of XRR experiments [see Fig. 1(b)] provided supporting evidence for the existence of two-layer and single-layer structures for adsorbed layers with thicknesses of ~10.4 and 3.0 nm, respectively. Combined, the present results suggest that the flattened layer of P(S-r-HS) constituting short loops of adsorbed chains is attainable after extensive solvent leaching.

Figure 2 shows the thickness of the fattened layers (h_F) as a function of f_{HS}. For $f_{HS} < 0.024$, h_F increased with increasing f_{HS}. For $0.024 < f_{HS} < 0.14$, h_F decreased with increasing f_{HS}, and for $f_{HS} > 0.14$, h_F was independent of the HS content. A quantitative relationship between h_F and f_{HS} could be determined based on the proposed nanolayers structure consisting of anchored HS and loop S segments, and it is given by Eq. (1) (see Fig. S4 in the SM [27] for details):

$$h_F = R\frac{104\sigma}{\rho f_{HS} N_a}, \tag{1}$$

where σ and ρ are the number of available anchoring points per unit area and mass density of h_F ($\rho = 1.13$ g/cm^3 determined by XRR), respectively; N_a stands for Avogadro's number; and R is a correction parameter reflecting the deviation from the proposed adsorption structure. As shown in Fig. 2, the data were quantitatively fit between $0.024 < f_{HS} < 0.14$ with $R = 0.85$ and $\sigma = 1.1$ nm^{-2}. For $0.024 < f_{HS}$ and $f_{HS} > 0.14$, the deviations in h_F from the model suggest adsorption of S at the interface and incorporation of HS segments in the loops of the flattened chains, respectively, and thus bound the f_{HS} values where the proposed local conformation of loops in the

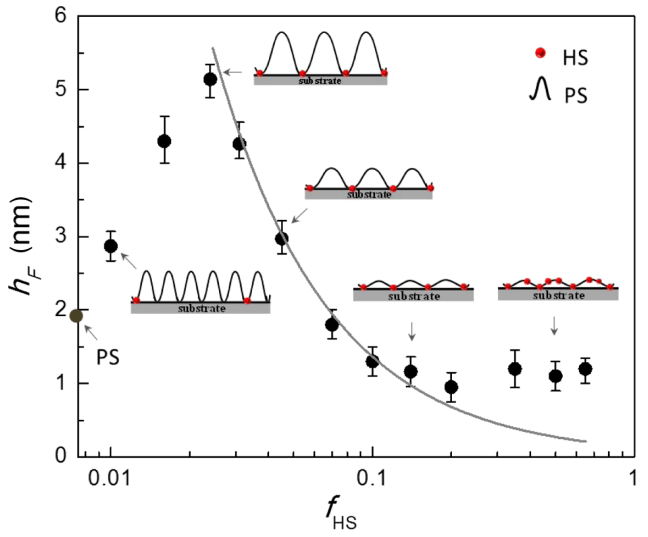

FIG. 2. h_F as a function of f_{HS}. (Inset) The proposed conformation of P(S-r-HS) flattened layers and the brown circle on the y axis is the h_F of PS. The curve is the fit by Eq. (1).

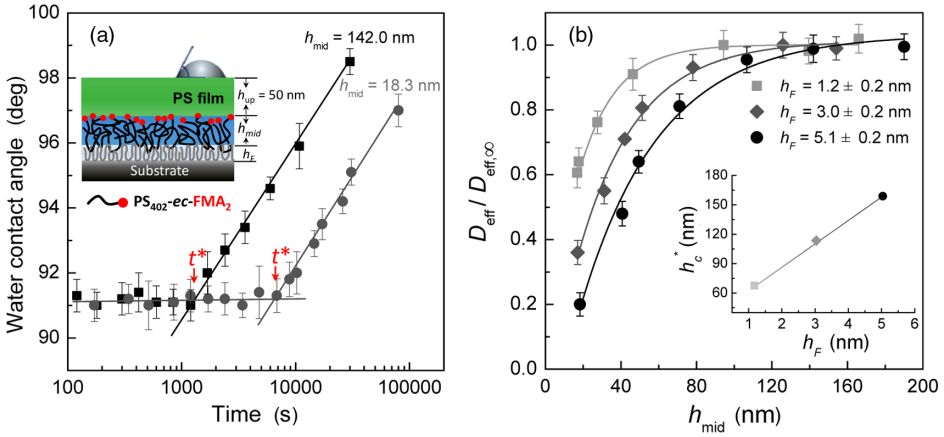

FIG. 3. (a) Water contact angle on a top PS surface as a function of annealing time ($h_F = 5.1$ nm; $T = 403$ K). (b) $D_{\mathrm{eff}}/D_{\mathrm{eff},\infty}$ as a function of h_{mid} ($T = 403$ K). The insets of (a) and (b) show the multilayer sample geometry and the relation between the h_c^* and h_F, respectively. The straight and curved lines are intended as guides for the eye.

flattened layers, as shown in Fig. 2, are valid. Further support for the proposed structure was obtained by a linear correlation between h_F and theoretical values of the loop height calculated by geometric analysis; see Figs. S5 and S6 in the SM [27]. AFM images in Fig. S7 in the SM [27] revealed smooth and consolidated adsorbed nanolayers atop the substrate, indicating the formation of a homogeneous loop structure of flattened chains atop the substrate surface. Taken together, the data presented above demonstrate that the height of loops in flattened layers can be controlled by altering f_{HS} provided that $0.024 < f_{\mathrm{HS}} < 0.14$.

The influence of adsorbed layer chain topology on diffusion in polystyrene (PS) thin films was obtained using a multilayer film geometry [34] recently developed to detect gradients of chain mobility near the interface by investigating the diffusion of a fluorinated tracer-labeled polymer [34]. A multilayer film [inset of Fig. 3(a)] composed of a bottom flattened layer of P(S-r-HS), a variable-thickness middle layer of polystyrene end capped with 2-perfluorooctylethyl methacrylate (FMA) units ($PS_{402}-ec-FMA_2$, $M_W = 43$ kg/mol, PDI = 1.12), and a top layer of PS ($h_{\mathrm{up}} = 50$ nm, $M_w = 40$ kg/mol, PDI = 1.08) was fabricated (see Sec. S5 of the SM [27] for sample preparations). Upon thermally annealing the multilayer film at 403 K ($T_g^{\mathrm{bulk}} + 30$ K), the fluorinated chains ($PS_{402} - ec - FMA_2$) diffuse through the top PS layer, eventually reaching the free surface. The critical time (t^*) required for $PS_{402} - ec - FMA_2$ chains to diffuse from the underlying interface to the topmost PS surface, which can be used to determine effective diffusion coefficients (D_{eff}, $D_{\mathrm{eff}} = h_{\mathrm{up}}^2/2t^*$, $h_{\mathrm{up}} = 50$ nm) based on Fick's law, were acquired by detecting the onset of water contact angle increment as a function of annealing time due to the enrichment of hydrophobic FMA units at the surface; see Fig. 3(a).

Figure 3(b) depicts the normalized diffusion coefficients ($D_{\mathrm{eff}}/D_{\mathrm{eff},\infty}$), where $D_{\mathrm{eff},\infty}$ is D_{eff} when the $PS_{402} - ec - FMA_2$ layer is sufficiently thick that the substrate does not influence the mobility of the chain at the $PS//PS_{402} - ec - FMA_2$ interface, as a function of the $PS_{402} - ec - FMA_2$ layer thickness (h_{mid}). Remarkably, for all films with adsorbed layers having different loop sizes in the flattened layers, $D_{\mathrm{eff}}/D_{\mathrm{eff},\infty}$ decreased significantly with a reduction in h_{mid} below a critical value. Since interfacial effects are known to cause long-range perturbations to molecular mobility and chain diffusion [8,15,20,21,35], the decrease in $D_{\mathrm{eff}}/D_{\mathrm{eff},\infty}$ is considered to result from interfacial effects exerting a greater influence on mobility as the middle layer thickness is reduced. In this context, the $D_{\mathrm{eff}}/D_{\mathrm{eff},\infty}$ vs h_{mid} curves represent the gradient distribution of chain mobility near the interface, and the value of h_c^*, defined as h_{mid} when $D_{\mathrm{eff}}/D_{\mathrm{eff},\infty} = 0.97$, were approximated as the critical length scale (or depth) over which a gradient in mobility, originating from interfacial effects at the substrate, could extend within a thin film. Interestingly, the h_c^* increased markedly with the loop height of the flattened chains; see the inset of Fig. 3(b). At $h_F = 5.1$ nm, the reduced thin film mobility persisted up to ~160 nm (i.e., $29R_g$)—a distance much larger than that of PS on bare silicon ($\sim 10R_g$) [8,34]. Our results illustrate that large loops of the flattened chains aid in the propagation of reduced interfacial molecular mobility.

We propose that the loops of the flattened chains provide a structure in which the neighboring unadsorbed chains can penetrate and become entangled, thus propagating suppressed dynamics of the adsorbed chain. To shed light on the changes of such topological interactions, we performed dewetting experiments of PS films (45 nm) atop P(S-r-HS) flattened layers (see experimental details in Sec. S6 in the SM [27]). Since loops of P(S-r-HS) flattened layers have the same chemical structures as the overlaying PS films, dewetting of the PS films from the adsorbed nanolayers is autophobic [36–41] in nature and driven by entropic

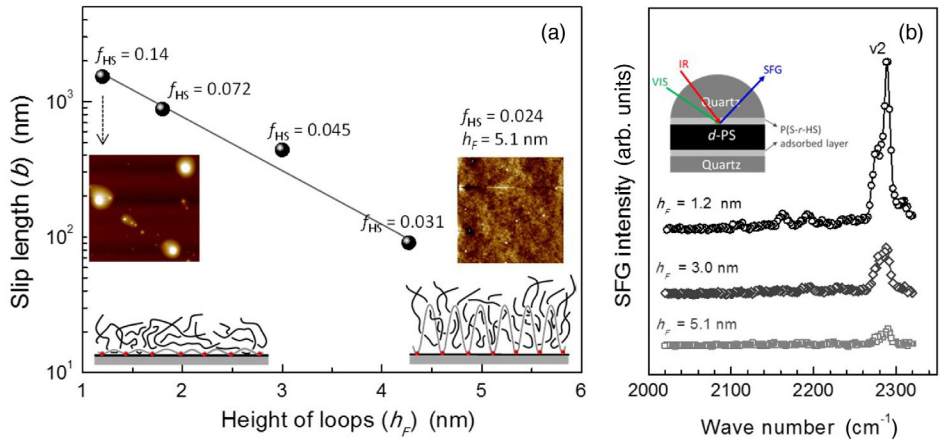

FIG. 4. (a) Slip length and AFM images of PS films on the adsorbed layers. (b) SFG spectra from the polymer-polymer interfaces between the adsorbed and the nonadsorbed chains. The insets of (a) and (b) illustrate the differences in interpenetration and entanglements formed between the adsorbed and neighboring free chains at low and high h_F and the sample geometry for SFG measurements, respectively. The size of the AFM images in (a) is 32×32 μm.

interaction, and dictated by the extent of chain interpenetration. Upon annealing at 423 K, the PS films readily dewet the adsorbed layers with $h_F \leq 4.2$ nm; however, the films remained stable on the adsorbed layers with $h_F = 5.1$ nm; see the Fig. 4(a) inset, consistent with the "wet" condition with strong interpenetration [39]. The relationship between the degree of interpenetration and loop height of the flattened chains was assessed by probing the interface slippage. Polymers can better slip at the interface with less interpenetration, while stronger interpenetration, associated with large interfacial friction, usually causes less slippage with a smaller slip length (b) [40–42]. The interfacial slip length (b) ($b \sim 1/k$, k: interfacial friction coefficients [40–42])—a parameter characterizing the degree of "slippiness"—of PS on the various adsorbed layers was evaluated by examining the dewetting dynamics (see Sec. S6 of the SM [27] for the calculations of b). It is evident that the slip length tends to decrease (indicating less slippiness) with increasing loop height of the flattened chains [see Fig. 4(a)], thus indicating the increased interfacial friction due to the formation of stronger interpenetrations and entanglements between loops in flattened layers and free chains in the matrix.

The interface of the flattened adsorbed layers was directly probed by a sum frequency generational spectroscopy (SFG). A sandwiched sample geometry, shown in the inset of Fig. 4(b) (see the sample preparations in Sec. S7 of the SM [27]), was used to acquire SFG signals from the interface of a deuterated PS film (d-PS) and underlying P(S-r-HS) adsorbed layers. When the loop height of flattened chains was small (e.g., $h_F = 1.2$ nm), strong signals in the C-D vibrational region from the phenyl ring of d-PS (i.e., v_2 at 2280 cm^{-1} [43]) appeared in the SFG spectra; see Fig. 4(b). However, the peak intensities decreased upon increasing height of the loops in the flattened adsorbed layers. Since the SFG signal is generated at an interface where the symmetry is broken and molecules are ordered [44], it could be reasonably inferred that a sharp and contrasting interface normally generates strong SFG signals; however a gradient and diffusive interface results in weak signals because of the loss of the molecular ordering at the interface [45]. Therefore, the SFG results also evidenced the notion that the flexible loops formed by the flattened chains facilitated the interpenetration and entanglements with the free chains in the matrix, and the strength of such topological interactions increased with an increase of the loop height.

Taken together, the results presented above demonstrate that the ability to tune the propagation of suppressed dynamics by a new parameter, i.e., the loop height of the flattened nanolayers, is essentially correlated to the topological interactions, which we regard as a result of the interpenetration and entanglement between the chains anchored to the surface and those without direct contact with the substrate. The increased topological interaction strenghthens the degree of motional coupling of chains, resulting in an increase in the distance of hindrance to interfacial dynamics with increasing loop height [Fig. 3(b)].

Finally, we show how the differences in absorbed nanolayer topology can be used to tune the T_g-confinement behavior of the PS films, i.e., a demonstration of exploiting confinement for property manipulation. As shown in Fig. 5, the T_g of thin PS films on the P(S-r-HS) adsorbed layer surface, as measured by ellipsometry, first decreases due to free surface effects [46,47] and then increases because of the dominance of the interfacial effect [46,47] with reduced film thickness. The threshold film thickness for the observed increase in T_g for the PS thin film is greater when placed atop adsorbed flattened nanolayers with larger loops, that is, 18, 26, and 33 nm for PS film on adsorbed layer with $h_F = 1.2$, 3.0, and 5.1 nm, respectively. We note that the nonmonotonic change in T_g, arising from the

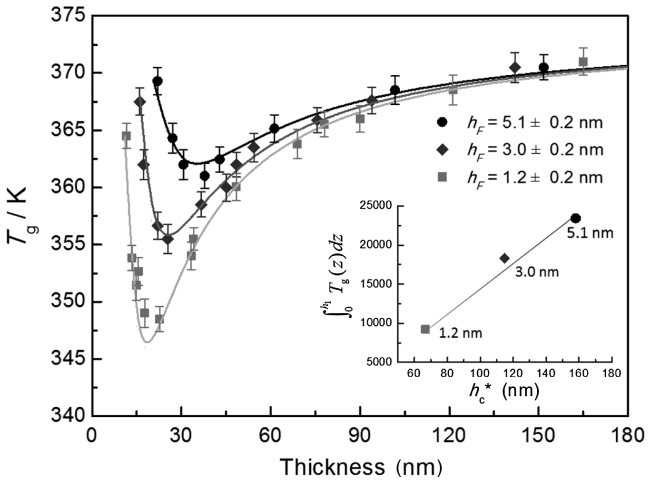

FIG. 5. T_g of PS films supported by the adsorbed layers as functions of the film thickness. (Inset) The linear correlations between $\int_0^{h_1} T_g(z)dz$ and h_c^*. The solid curves represent the best fitting of the T_g using the three-layer model [Eq. (2)] to extract $\int_0^{h_1} T_g(z)dz$.

counteraction between interface and free surface effects, was previously observed for PS-COOH on SiO_x, but the increase in T_g occurred at much smaller thicknesses (i.e., <10 nm) [48,49]. The larger threshold values indicate that the loop structures of the P(S-r-HS) flattened chains which aid the propagation of suppressed interfacial dynamics amplify the influence of the interfacial effect. The contribution of interfacial effects on T_g of PS films was extracted by fitting $T_g(h)$ vs thickness curves (see Fig. 5) using a three-layer model containing a surface mobile layer, a bulk region, and an interfacial layer [47,50,51]:

$$T_g(h) = \frac{h - h_1}{h} T_g^{\text{bulk}} \left[1 - \left(\frac{\gamma}{h}\right)^{\delta}\right] + \frac{\int_0^{h_1} T_g(z)dz}{h}. \quad (2)$$

The first term in Eq. (2) reflects the effects of a mobile free surface, in which γ and δ are surface-related parameters ($\gamma = 3.2 \pm 0.6$ nm, $\delta = 1.8 \pm 0.2$ for PS) [50,51]; h_1 is the thickness of the interfacial layers. The second term accounts for the contribution of suppressed interfacial dynamics, in which $T_g(z)$ is a function describing the depth distribution of local T_g, and the integration $[\int_0^{h_1} T_g(z)dz]$ is the sum of $T_g(z)$ of all of the sublayers with different distances from the adsorbed layers. It was shown that the integral term increases with increasing loop height of the flattened chain, as shown in the inset of Fig. 5. Moreover, $\int_0^{h_1} T_g(z)dz$ correlates linearly with the distance at which the substrate affects polymer mobility (h_c^*); see Fig. 5. Figure 5 also illustrates that both h_c^* and T_g of the PS thin film increased with the thickness of the flattened layer. This behavior is qualitatively consistent with that reported in homopolymers [12,13], in which a correlation between the adsorbed amount and the material properties was identified, and therefore further supports the claim that the chain adsorption governs the equilibrium and nonequilibrium dynamics of confined polymers.

This Letter points to new physics in understanding interfacial effects on relaxation dynamics of the nanoconfined polymers: the local conformation of chains adsorbed atop solid surfaces plays a vital role on the propagation of suppressed dynamics induced by interacting substrates, by altering topological interactions of chains at the polymer-polymer interface with the adsorbed structure of chains closest to the substrate. The flattened adsorbed chains with larger loops are highly efficient in propagating suppressed interfacial dynamics because of their ease in forming strong topological constraints with free chains, giving rise to interfacial effects which can be propagated far from the substrate. The results of this Letter enable us with an opportunity to tune the length scale that interfacial effects propagate by using the rationalized optimization of the local conformation, and more specifically the size of the loops, of the adsorbed flattened chains on solid surfaces, and they thus have strong implications for reinforced polymer nanocomposites, where the filler-polymer interface is believed to be important.

We acknowledge financial support from Natural Science Foundation of China (Grants No. 21504081 and No. 21674100) and the National Science Foundation (NSF) Materials Research Science and Engineering Center Program through the Princeton Center for Complex Materials (Grant No. DMR-1420541). R. D. P. acknowledges the NSF through Grant No. CBET-1706012.

*Corresponding author.
wxinping@zstu.edu.cn
†Corresponding author.
rpriestl@princeton.edu
‡Corresponding author.
chemizuo@zstu.edu.cn

[1] M. Alcoutlabi and G. B. McKenna, Effects of confinement on material behaviour at the nanometre size scale, J. Phys. Condens. Matter **17**, R461 (2005).
[2] M. D. Ediger and J. A. Forrest, Dynamics near free surfaces and the glass transition in thin polymer films: A view to the future, Macromolecules **47**, 471 (2014).
[3] S. Napolitano, E. Glynos, and N. B. Tito, Glass transition of polymers in bulk, confined geometries, and near interfaces, Rep. Prog. Phys. **80**, 036602 (2017).
[4] R. D. Priestley, C. J. Ellison, L. J. Broadbelt, and J. M. Torkelson, Structural relaxation of polymer glasses at surfaces, interfaces, and in between, Science **309**, 456 (2005).
[5] Z. Yang, Y. Fujii, F. K. Lee, C-H. Lam, and O. K. C. Tsui, Glass transition dynamics and surface layer mobility in unentangled polystyrene films, Science **328**, 1676 (2010).

[6] C. J. Ellison and J. M. Torkelson, The distribution of glass-transition temperatures in nanoscopically confined glass formers, Nat. Mater. **2**, 695 (2003).
[7] A. Papon, H. Montes, M. Hanafi, F. Lequeux, L. Guy, and K. Saalwachter, Glass-Transition Temperature Gradient in Nano-Composites: Evidence from Nuclear Magnetic Resonance and Differential Scanning Calorimetry, Phys. Rev. Lett. **108**, 065702 (2012).
[8] X. Zheng, M. H. Rafailovich, J. Sokolov, Y. Strzhemechny, S. A. Schwarz, B. B. Sauer, and M. Rubinstein, Long-Range Effects on Polymer Diffusion Induced by a Bounding Interface, Phys. Rev. Lett. **79**, 241 (1997).
[9] D. Long and F. Lequeux, Heterogeneous dynamics at the glass transition in van der Waals liquids, in the bulk and in thin films, Eur. Phys. J. E **4**, 371 (2001).
[10] A. Papon, K. Saalwächter, K. Schäler, L. Guy, F. Lequeux, and H. Montes, Low-field NMR investigations of nanocomposites: Polymer dynamics and network effects, Macromolecules **44**, 913 (2011).
[11] S. Napolitano and M. Wübbenhorst, The lifetime of the deviations from bulk behavior in polymers confined at the nanoscale, Nat. Commun. **2**, 260 (2011).
[12] A. Panagopoulou and S. Napolitano, Irreversible Adsorption Governs the Equilibration of Thin Polymer Films, Phys. Rev. Lett. **119**, 097801 (2017).
[13] N. G. Perez-de-Eulate, M. Sferrazza, D. Cangialosi, and S. Napolitano, Irreversible adsorption erases the free surface effect on the T_g of supported films of poly(4-tert-butylstyrene), ACS Macro Lett. **6**, 354 (2017).
[14] D. N. Simavilla, W. Huang, C. Housmans, M. Sferrazza, and S. Napolitano, Taming the strength of interfacial interactions via nanoconfinement, ACS Cent. Sci. **4**, 755 (2018).
[15] T. Koga, N. Jiang, P. Gin, M. K. Endoh, S. Narayanan, L. B. Lurio, and S. K. Sinha, Impact of an Irreversibly Adsorbed Layer on Local Viscosity of Nanoconfined Polymer Melts, Phys. Rev. Lett. **107**, 225901 (2011).
[16] J. Xu, Z. Liu, Y. Lan, B. Zuo, X. Wang, J. Yang, W. Zhang, and W. Hu, Mobility gradient of poly(ethylene terephthalate) chains near a substrate scaled by the thickness of the adsorbed layer, Macromolecules **50**, 6804 (2017).
[17] S. Sun, H. Xu, J. Han, Y. Zhu, and B. Zuo, X. Wang, and W. Zhang, The architecture of the adsorbed layer at the substrate interface determines the glass transition of supported ultrathin polystyrene films, Soft Matter **12**, 8348 (2016).
[18] B. Zuo, J. Xu, S. Sun, Y. Liu, J. Yang, L. Zhang, and X. Wang, Stepwise crystallization and the layered distribution in crystallization kinetics of ultra-thin poly(ethylene terephthalate) film, J. Chem. Phys. **144**, 234902 (2016).
[19] M. J. Burroughs, S. Napolitano, D. Cangialosi, and R. D. Priestley, Direct measurement of glass transition temperature in exposed and buried adsorbed polymer nanolayers, Macromolecules **49**, 4647 (2016).
[20] N. Jiang, L. Sendogdular, X. Di, M. Sen, P. Gin, M. K. Endoh, T. Koga, B. Akgun, M. Dimitriou, and S. Satija, Effect of CO_2 on a mobility gradient of polymer chains near an impenetrable solid, Macromolecules **48**, 1795 (2015).
[21] M. Krutyeva, A. Wischnewski, M. Monkenbusch, L. Willner, J. Maiz, C. Mijangos, A. Arbe, J. Colmenero, A. Radulescu, O. Holderer, M. Ohl, and D. Richter, Effect of Nanoconfinement on Polymer Dynamics: Surface Layers and Interphases, Phys. Rev. Lett. **110**, 108303 (2013).
[22] K. Motomura and R. Matuura, Conformation of adsorbed polymeric chain. II,, J. Chem. Phys. **50**, 1281 (1969).
[23] G. J. Fleer, M. A. Cohen-Stuart, J. M. H. M. Scheutjens, T. Cosgrove, and B. Vincent, *Polymers at Interfaces* (Chapman and Hall, London, 1993).
[24] P. Gin, N. Jiang, C. Liang, T. Taniguchi, B. Akgun, S. K. Satija, M. K. Endoh, and T. Koga, Revealed Architectures of Adsorbed Polymer Chains at Solid-Polymer Melt Interfaces, Phys. Rev. Lett. **109**, 265501 (2012).
[25] N. Jiang, J. Shang, X. Di, M. K. Endoh, and T. Koga, Formation mechanism of high-density, flattened polymer nanolayers adsorbed on planar solids, Macromolecules **47**, 2682 (2014).
[26] S. Cheng, A. P. Holt, H. Wang, F. Fan, V. Bocharova, H. Martin, T. Etampawala, B. T. White, T. Saito, N-G. Kang, M. D. Dadmun, J. W. Mays, and A. P. Sokolov, Unexpected Molecular Weight Effect in Polymer Nanocomposites, Phys. Rev. Lett. **116**, 038302 (2016).
[27] See Supplemental Material at http://link.aps.org/supplemental/10.1103/PhysRevLett.122.217801, which includes Refs. [28–30] for (1) synthesis of the P(S-r-HS) copolymers, (2) deducing the quantitative relation between h_F and f_{HS}, (3) estimation of h_{Theo}, (4) AFM images of the P(S-r-HS) adsorbed layers, (5) preparation of the multilayer films used for diffusion measurement, (6) determination of the slip length, and (7) basic principle and experimental details for the SFG measurements
[28] F. Brochard-Wyart, P.-G. de Gennes, H. Hervert, and C. Redon, Wetting and slippage of polymer melts on semi-ideal surfaces, Langmuir **10**, 1566 (1994).
[29] F. Vidal and A. Tadjeddine, Sum-frequency generation spectroscopy of interfaces, Rep. Prog. Phys. **68**, 1095 (2005).
[30] B. Zuo, M. Inutsuka, D. Kawaguchi, X. Wang, and K. Tanaka, Conformational relaxation of poly(styrene-co-butadiene) chains at substrate interface in spin-coated and solvent-cast films, Macromolecules **51**, 2180 (2018).
[31] M. M. Vaidya, K. Levon, and E. M. Pearce, Miscibility of poly (ε- caprolactone), a semicrystalline polymer, with amorphous poly (styrene-4-hydroxystyrene) copolymers, J. Polym. Sci. Polym. Phys. **33**, 2093 (1995).
[32] K. J. Zhu, S. F. Chen, T. Ho, E. M. Pearce, and T. K. Kwei, Miscibility of copolymer blends, Macromolecules **23**, 150 (1990).
[33] R. S. Tate, D. S. Fryer, S. Pasqualini, M. F. Montague, J. J. de Pablo, and P. F. Nealey, Extraordinary elevation of the glass transition temperature of thin polymer films grafted to silicon oxide substrates, J. Chem. Phys. **115**, 9982 (2001).
[34] J. Xu, Y. Zhang, H. Zhou, Y. Hong, B. Zuo, X. Wang, and L. Zhang, Probing the utmost distance of polymer dynamics suppression by a substrate by investigating the diffusion of fluorinated tracer-labeled polymer chains, Macromolecules **50**, 5905 (2017).
[35] R. Inoue, M. Nakamura, K. Matsui, T. Kanaya, K. Nishida, and M. Hino, Distribution of glass transition temperature in multilayered poly(methyl methacrylate) thin film supported on a Si substrate as studied by neutron reflectivity. Phys. Rev. E **88**, 032601 (2013).

[36] G. Reiter, J. Schultz, P. Auroy, and L. Auvray, Improving adhesion via connector polymers to stabilize non-wetting liquid films, Europhys. Lett. **33**, 29 (1996).
[37] L. Leibler and A. Mourran, Wetting on grafted polymer films, MRS Bull. **22**, 33 (1997).
[38] P. G. Ferreira, A. Ajdari, and L. Leibler, Scaling law for entropic effects at interfaces between grafted layers and polymer melts, Macromolecules **31**, 3994 (1998).
[39] H. Oh and P. F. Green, Polymer chain dynamics and glass transition in athermal polymer/nanoparticle mixtures, Nat. Mater. **8**, 139 (2009).
[40] G. Reiter and R. Khanna, Real-Time Determination of the Slippage Length in Autophobic Polymer Dewetting, Phys. Rev. Lett. **85**, 2753 (2000).
[41] G. Reiter and R. Khanna, Kinetics of autophobic dewetting of polymer films, Langmuir **16**, 6351 (2000).
[42] R. Fetzer, M. Rauscher, A. Munch, B. A. Wagner, and K. Jacobs, Slip-controlled thin-film dynamics, Europhys. Lett. **75**, 638 (2006).
[43] Y. Hong, Y. Li, F. Wang, B. Zuo, X. Wang, L. Zhang, D. Kawaguchi, and K. Tanaka, Enhanced thermal stability of polystyrene by interfacial noncovalent interactions, Macromolecules **51**, 5620 (2018).
[44] Y. R. Shen, Surface properties probed by second-harmonic and sum-frequency generation, Nature (London) **337**, 519 (1989).
[45] J. Wang, C. L. Loch, D. Ahn, and Z. Chen, Demonstrating the feasibility of monitoring the molecular-level structures of moving polymer/silane interfaces during silane diffusion using SFG, J. Am. Chem. Soc. **126**, 1174 (2004).
[46] M. Campoy-Quiles, M. Sims, P. G. Etchegoin, and D. D. C. Bradley, Thickness-dependent thermal transition temperatures in thin conjugated polymer films, Macromolecules **39**, 7673 (2006).
[47] D. Liu, R. O. Orozco, and T. Wang, Deviations of the glass transition temperature in amorphous conjugated polymer thin films, Phys. Rev. E **88**, 022601 (2013).
[48] J. L. Keddie and R. A. L. Jones, Glass transition behavior in ultra-thin polystyrene films, Isr. J. Chem. **35**, 21 (1995).
[49] J. A. Forrest and J. Mattsson, Reductions of the glass transition temperature in thin polymer films: Probing the length scale of cooperative dynamics, Phys. Rev. E **61**, R53(R) (2000).
[50] J. L. Keddie, R. A. L. Jones, and R. A. Cory, Size-dependent depression of the glass transition temperature in polymer films, Europhys. Lett. **27**, 59 (1994).
[51] J. L. Keddie, R. A. L. Jones, and R. A. Cory, Interface and surface effects on the glass-transition temperature in thin polymer films, Faraday Discuss. **98**, 219 (1994).